



Electrocatalytic activity and stability of carbon nanotubes-supported Pt-on-Au, Pd-on-Au, Pt-on-Pd-on-Au, Pt-on-Pd, and Pd-on-Pt catalysts for methanol oxidation reaction



Ranran Shi^a, Jianshe Wang^{a,b,*}, Niancai Cheng^b, Xueliang Sun^b, Lei Zhang^c,
Jiujun Zhang^c, Liucheng Wang^a

^a School of Chemical Engineering and Energy, Zhengzhou University, Zhengzhou 450000, PR China

^b Department of Mechanical and Materials Engineering, The University of Western Ontario, ON N6A 5B9, Canada

^c Energy, Mining & Environment, National Research Council of Canada, Vancouver, BC V6 T 1W5, Canada

ARTICLE INFO

Article history:

Received 19 August 2014

Received in revised form 9 October 2014

Accepted 9 October 2014

Available online 14 October 2014

Keywords:

methanol oxidation
low-Pt catalysts
stability
activity
Pt-on-Pd

ABSTRACT

For optimizing both the activity and stability of Pt-based catalysts for methanol oxidation reaction (MOR), several carbon nanotubes (CNTs)-supported catalysts such as Pt-on-Au/CNTs, Pd-on-Au/CNTs, Pt-on-Pd-on-Au/CNTs, Pt-on-Pd/CNTs, and Pd-on-Pt/CNTs catalysts are synthesized mainly through electrodeposition method. The activity and stability comparisons show that Pt-on-Au/CNTs has a higher MOR activity but a lower stability than Pd-on-Au/CNTs. To utilize the merits of the Pt and Pd components, Pt-on-Pd-on-Au/CNTs and Pt-on-Pd/CNTs catalysts are synthesized. The Pt-on-Pd-on-Au/CNTs and Pt-on-Pd/CNTs catalysts shows higher MOR activity than Pd-on-Au/CNTs and Pd/CNTs catalysts and higher stability than Pt-on-Au/CNTs, suggesting a synergistic interaction between Pt and Pd in catalyzing methanol oxidation reaction. Calculation shows that the total mass activity of Pt-on-Pd/CNTs with quite low Pt amount is on a similar level as that of Pt/CNTs for MOR oxidation, indicating the Pt-on-Pd catalyst could have promising potential as a low-Pt catalyst for MOR in alkaline media.

© 2014 Elsevier Ltd. All rights reserved.

1. Introduction

The polymer electrolyte membrane fuel cells (PEMFCs) using hydrogen and air (oxygen) gases as reactants can produce clean electrical power with high energy efficiency for portable, stationary and automobile power applications [1–3]. A member of the PEMFCs family, direct methanol fuel cell (DMFC) using methanol as fuel and air (oxygen) as oxidant, and featuring higher energy density and more convenient fuel supply, has been recognized as one of the most feasible and practical options for commercialization [4–6]. However, the anode methanol oxidation reaction (MOR) in acid media highly depends on Pt-containing catalysts, in which the Pt component is of high cost and low abundance. Moreover, the Pt surface can be easily poisoned by strongly adsorbed intermediates, leading to slow methanol oxidation kinetics and then large electrode overpotential [7,8]. Furthermore, the kinetics of DMFC cathode oxygen reduction reaction (ORR) in acid media

[9,10] is also sluggish, leading to a low performance. In contrast to the case in acid media, both MOR [11–13] and ORR [14,15] can proceed with enhanced activity in alkaline media. Therefore, a considerable research attention has been shifted to alkaline polymer electrolyte membrane fuel cells (APEMFC) in recent years [16–18].

Regarding the electrocatalysis in APEMFCs, low-Pt [19,20] and non-Pt [21–24] catalysts have been the major research targets for further improving the reaction kinetics. Particularly, due to the significantly lower apparent activation energy of MOR on Pt catalysts in alkaline media than that in acidic media [25], using low-Pt and even non-Pt catalysts becomes possible. Among various kinds of low-Pt catalysts explored, Pt-on-Au catalyst [19,26,27] has been reported to be highly active for MOR in alkaline media. However, our previous work [26] showed that the MOR activity on Pt-on-Au catalyst could be decreased quickly during the stability test, suggesting that the stability of Pt-on-Au catalyst needs to be further improved in order to meet the requirement of practical applications. On the other hand, Pd-based catalysts [28–31] towards MOR in alkaline media are widely explored as the non-Pt catalysts due to Pd's relatively lower cost and similar property to those of Pt-based catalysts. Up to now, most researches focus on

* Corresponding author. Tel.: +86 0371 67781027; fax: +86 0371 67781027.
E-mail addresses: wangjs07@zzu.edu.cn (J. Wang), wanglc@zzu.edu.cn (L. Wang).

the MOR kinetics of Pd-based catalysts to improve their catalytic activities, and there are only limited work reported on the stability of Pd-based catalysts [30,31].

To address the low stability challenge of Pt-on-Au catalyst and explore the possibility that Pd can be used as a cheaper and stable candidate to Pt (or Au), in this paper, we firstly compared Pd-on-Au with Pt-on-Au catalysts and found that the Pd-on-Au has higher stability than Pt-on-Au while the Pt-on-Au has much higher activity than Pd-on-Au counterpart. To optimize both activity and stability, we further prepared Pt-on-Pd catalyst. Interestingly, the catalytic activity of this Pt-on-Pd catalyst toward methanol oxidation reaction were found to be greatly improved in comparison with the Pd catalyst without Pt modification, and the stability of Pt-on-Pd was also superior to that of Pt-on-Au counterpart. Structural characterizations using electrochemical methods were conducted for understanding the structure-property relationship during MOR electrocatalysis. We believe this understanding will be meaningful for future catalyst development.

2. Experimental

Multi-walled carbon nanotubes (CNTs) were obtained from Shenzhen Nanotech Port Co. Ltd and purified before use. $\text{H}_2\text{PtCl}_6 \cdot 6\text{H}_2\text{O}$, $\text{HAuCl}_4 \cdot 4\text{H}_2\text{O}$, PdCl_2 , K_2PtCl_4 and other reagents were all of analytical purity.

The first step for catalyst synthesis was to prepare Au/CNTs precursor (CNTs supported Au particles) through chemical reducing of $\text{HAuCl}_4 \cdot 4\text{H}_2\text{O}$ in alkaline ethylene glycol (EG) solution containing CNTs [26]. Briefly, 80 mg CNTs were ultrasonically dispersed in 80 mL EG solution containing 400 mg NaOH to form Solution I, and another 20 mL EG solution containing 41.8 mg $\text{HAuCl}_4 \cdot 4\text{H}_2\text{O}$ in the absence of CNTs was prepared to form Solution II. After mixing the two Solutions I and II under magnetic stirring for 30 minutes, the formed mixture was neutralized with aqueous HCl solution, filtrated, washed and then oven dried to obtain Au/CNTs precursor with a designed Au content of 20 wt.%. The X-ray diffraction (XRD) patterns of Au/CNTs were recorded on a Rigaku X-ray diffractometer (X' Pert PRO, Panalytical Company, Netherlands) using Cu-K α as radiation source. The morphology of Au/CNTs was investigated using transmission electron microscopy (TEM).

In this paper, in total five catalysts were prepared: Pt-on-Au/CNTs, Pd-on-Au/CNTs, Pt-on-Pd-on-Au/CNTs, Pt-on-Pd/CNTs, and Pd-on-Pt/CNTs. For electrochemical preparation of these catalysts

and their electrochemical characterization, a three-electrode cell coupled with a CHI electrochemical workstation (CHI 660, Shanghai Chenhua Instrument CO., Ltd. China) was used. A glassy carbon electrode (GC, $\Phi=3$ mm), a Pt wire electrode and a saturated calomel electrode (SCE) were used as the working electrode, counter electrode and reference electrode, respectively. The distance between the working electrode and counter electrode was about 6 mm. All potentials in this report were referred to SCE, and all the electrochemical experiments were conducted under 25 °C.

Pt-on-Au/CNTs and Pd-on-Au/CNTs. The preparation of Pt-on-Au/CNTs and Pd-on-Au/CNTs followed a site-selective electrodeposition procedure reported previously [26,32], the major advantage of which is the simple and facile manipulation without using reduction agent or protecting agent [33]. Moreover, the site-selectivity of Pt or Pd deposition could be achieved under milder condition in shorter time in contrast to chemical method [34]. The electrodeposition of Pt on CNTs-supported-Au was conducted at 0.65 V for 200 seconds on a Au/CNTs electrode in 1 M HClO_4 + 1 mM H_2PtCl_6 aqueous solution saturated by N_2 gas. The potential of Pd deposition (200 seconds) on CNTs-supported-Au was determined to be 0.6 V in 1 M HClO_4 + 1 mM H_2PdCl_4 aqueous solution saturated by N_2 gas, where H_2PdCl_4 was pre-prepared by dissolving 1 g PdCl_2 in 3 mL HCl (36.5 wt.%).

Pt-on-Pd-on-Au/CNTs. For electrochemical preparation of Pt-on-Pd-on-Au/CNTs (the Pd being deposited on Au and then the Pt being deposited on Pd), Pd-on-Au/CNTs was first prepared at 0.6 V for 4000 seconds in 1 M HClO_4 + 1 mM H_2PdCl_4 aqueous solution saturated by N_2 gas, and then Pt deposition at 0.6 V for 20 seconds was achieved in 1 M HClO_4 + 1 mM K_2PtCl_4 aqueous solution saturated by N_2 gas. The reason why the time range is long for Pd deposition while short for Pt deposition is that a high coverage Pd surface could thus form over Au surface and then the Pt moieties could deposit on Pd forming the Pt-on-Pd structure.

Pt-on-Pd/CNTs. To clearly verify the effect of Pd without the involvement of Au, Pd/CNTs (Pd supported on CNTs) was also prepared through constant-potential Pd deposition at 0.4 V for 600 seconds. After a CNTs/GC electrode (GC coated with 0.1 mg CNTs) being prepared by pipetting CNTs-containing ink on a GC electrode and dried for a half of an hour at 90 °C, the CNTs/GC electrode was scanned in 1 M HClO_4 aqueous solution saturated by N_2 gas until a steady cyclic voltammograms (CVs) was recorded. Then the CNTs/GC electrode was immersed in 1 M HClO_4 + 1 mM H_2PdCl_4 aqueous solution saturated by N_2 gas for constant potential deposition of 600 seconds. Then Pt-on-Pd/CNTs was

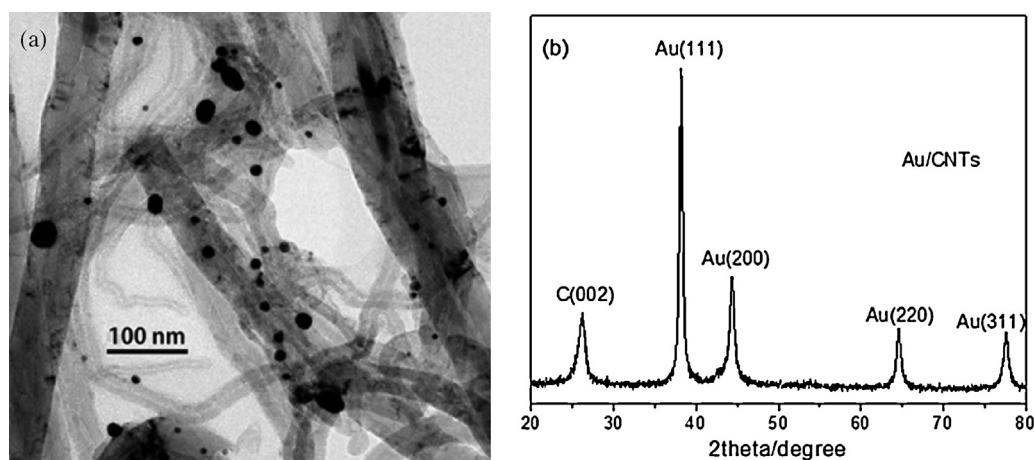


Fig. 1. (a) TEM and (b) XRD patterns of Au/CNTs.

prepared through constant potential deposition at 0.6 V for 20 seconds following the same electrodeposition procedure as above.

Pd-on-Pt/CNTs. Pd-on-Pt/CNTs (Pd being deposited on CNTs-supported Pt) was also prepared for observing the synergistic interaction between Pd and Pt during methanol oxidation in alkaline media. A GC disk electrode coated with 0.1 mg as-prepared Pt/CNTs [35] was immersed in 1 mol L⁻¹ HClO₄ solution with N₂ purging for 20 minutes. Steady CVs were recorded after 20 cycles of sweeping at 50 mV s⁻¹, followed by potentiostatic deposition at 0.6 V in 1 M HClO₄ + 1 mM H₂PdCl₄ aqueous solution saturated by N₂ gas.

The electrochemical data for all catalysts were recorded until steady state reached. The stability of all catalysts was investigated by cyclic voltammetric sweeping in 1 M NaOH + 1 M CH₃OH solution for certain cycles to record the decay of peak current of methanol oxidation. Other tests including linear sweeping voltammetry (LSV) and chronoamperometry were conducted prior to the stability test.

3. Results and Discussion

3.1. Comparisons of Pt-on-Au/CNTs and Pd-on-Au/CNTs in terms of activity and stability

Our previous study [26] showed that the structural stability of Pt-on-Au catalyst might need further improvement although they exhibited high activity for methanol oxidation. To assess the possibility of substituting Pd for Pt in Pt-on-Au/CNTs catalysts, we herein prepared Pd-on-Au/CNTs and compared it with Pt-on-Au/CNTs in terms of both methanol oxidation activity and stability.

The Au/CNTs was firstly prepared and characterized using both TEM and XRD, as shown in Fig. 1. The TEM image indicates that the Au particles with wide size distribution have been successfully deposited on the surface of CNTs. From the XRD patterns of Au/CNTs, it can be assigned that the peak at 26° is associated with C (002) and the peaks at 38.3°, 44.4°, 64.7°, 77.6° can be ascribed to Au(111), Au(200), Au(220) and Au(311), respectively [36]. The above results confirm the formation of Au/CNTs.

Pt-on-Au/CNTs and Pd-on-Au/CNTs were prepared through constant-potential deposition of H₂PtCl₆ at 0.65 V and H₂PdCl₄ at 0.6 V, respectively, and the deposition currents are shown in Fig. 2(a). The average deposition current for Pt and Pd is about 0.00064 mA, and the blank current for Pt (*I*_{blank-1}) and Pd (*I*_{blank-2})

deposition is about 0.00049 mA and 0.00040 mA, respectively. The net current for Pt deposition and Pd deposition is calculated to be about 0.00015 mA and 0.00024 mA, respectively. Taking 0.505 mg_{Pt}C⁻¹ and 0.549 mg_{Pd}C⁻¹ (obtained according to the Faraday Law) as references [26], the mass of Pt and Pd after 200 seconds of deposition can be calculated to be 1.5 × 10⁻⁵ mg_{Pt} and 2.6 × 10⁻⁵ mg_{Pd}, respectively.

To investigate the structural changes after Pt and Pd deposition onto the Au/CNTs, the linear sweep voltammetry (LSV) curves of Pt-on-Au/CNTs, Pd-on-Au/CNTs and Au/CNTs were recorded, as shown in Fig. 2(b). It can be seen that the Au oxide reduction peak area were decreased after Pt or Pd deposition, indicating that the Au surfaces are partly covered by Pt or Pd. In the upper graph in Fig. 2(b) a new peak at 0.7 V appears that can be ascribed to Pd oxide reduction [37], further indicating the formation of Pd-on-Au structure. Herein the Pd oxide reduction peak lies in a relatively higher value, mainly because the scanning rate is low and the Pd amount is small.

The electrochemical activity and stability of Pd-on-Au/CNTs were tested in comparison with Pt-on-Au/CNTs, as shown in Fig. 3(a). It is obvious that the Au/CNTs has no MOR activity. After Pt or Pd deposition on Au, there appears evident peak current of methanol oxidation on Pt-on-Au/CNTs or Pd-on-Au/CNTs. However, the activity of the former is evidently higher than that of the latter. The chronoamperometry data also supports this conclusion, as shown in Fig. 3(b). According to the peak current of MOR on Pt-on-Au/CNTs (~1.0 mA) or Pd-on-Au/CNTs (~0.1 mA) catalyst and the Pt or Pd mass, the Pt mass activity of the Pt-on-Au/CNTs and Pd-on-Au/CNTs is calculated to be 66.7 A mg_{Pt}⁻¹ and 3.8 A mg_{Pd}⁻¹, respectively, indicating a higher activity of Pt-on-Au than Pd-on-Au catalyst. In fact, Zhang et. al [27] have also reported a high activity (70 A mg_{Pt}⁻¹) of Pt-on-Au catalyst for methanol oxidation, further confirming the important role of low amount of Pt to modify the Au substrate. Considering that the Au metal is also expensive, the total mass activity was calculated for Pt-on-Au and Pd-on-Au, which is 50 mA mg_(Pt+Au)⁻¹ and 5 mA mg_(Pd+Au)⁻¹, respectively.

The reason for the higher activity of Pt-on-Au/CNTs than Pd-on-Au/CNTs might be related to different tendencies of OH_{ad} formation on Pt and Pd surface. As seen in Fig. 3(c), the current for Pt-OH formation (see the lower graph) is evidently higher than that for Pd-OH formation (see the upper graph). Considering the Pt amount being lower than Pd as calculated above, it can be assumed that the Pt-OH formation is easier than Pd-OH. Because

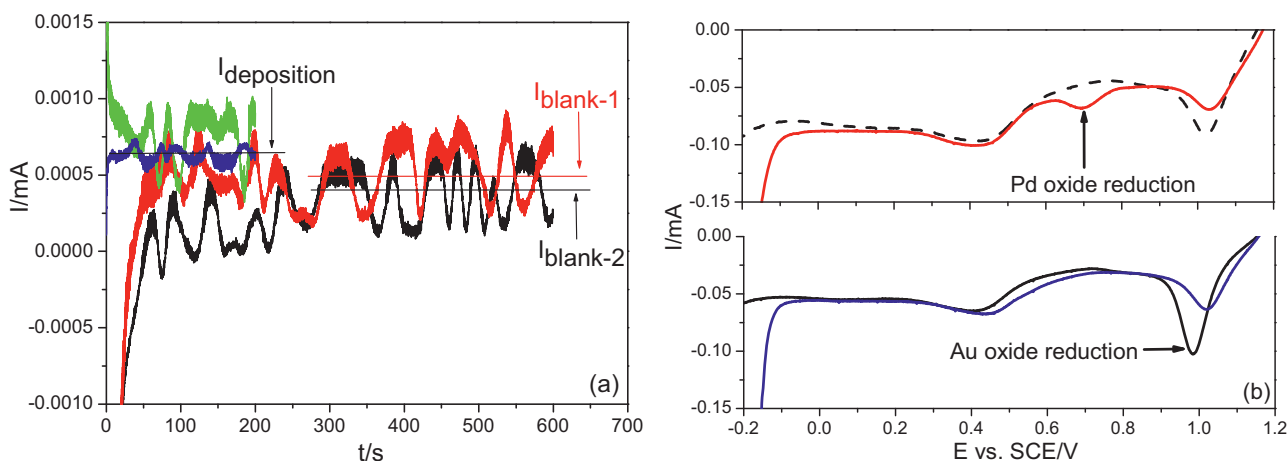


Fig. 2. (a) Deposition currents of Pt and Pd on Au/CNTs (~0.1 mg) together with corresponding blank currents for comparison; the average current for Pt deposition (blue line) and Pd deposition (green line) is 0.00064 mA, and the blank current for Pt and Pd deposition is 0.00049 mA and 0.00040 mA, respectively. (b) Linear sweeping voltammetry (LSV) curves recorded on Pt-on-Au/CNTs (blue solid line in lower graph) and Pd-on-Au/CNTs (red solid line in upper graph) in 1 M HClO₄ with corresponding LSV curves on Au/CNTs as references. Potential scan rate: 0.05 V s⁻¹.

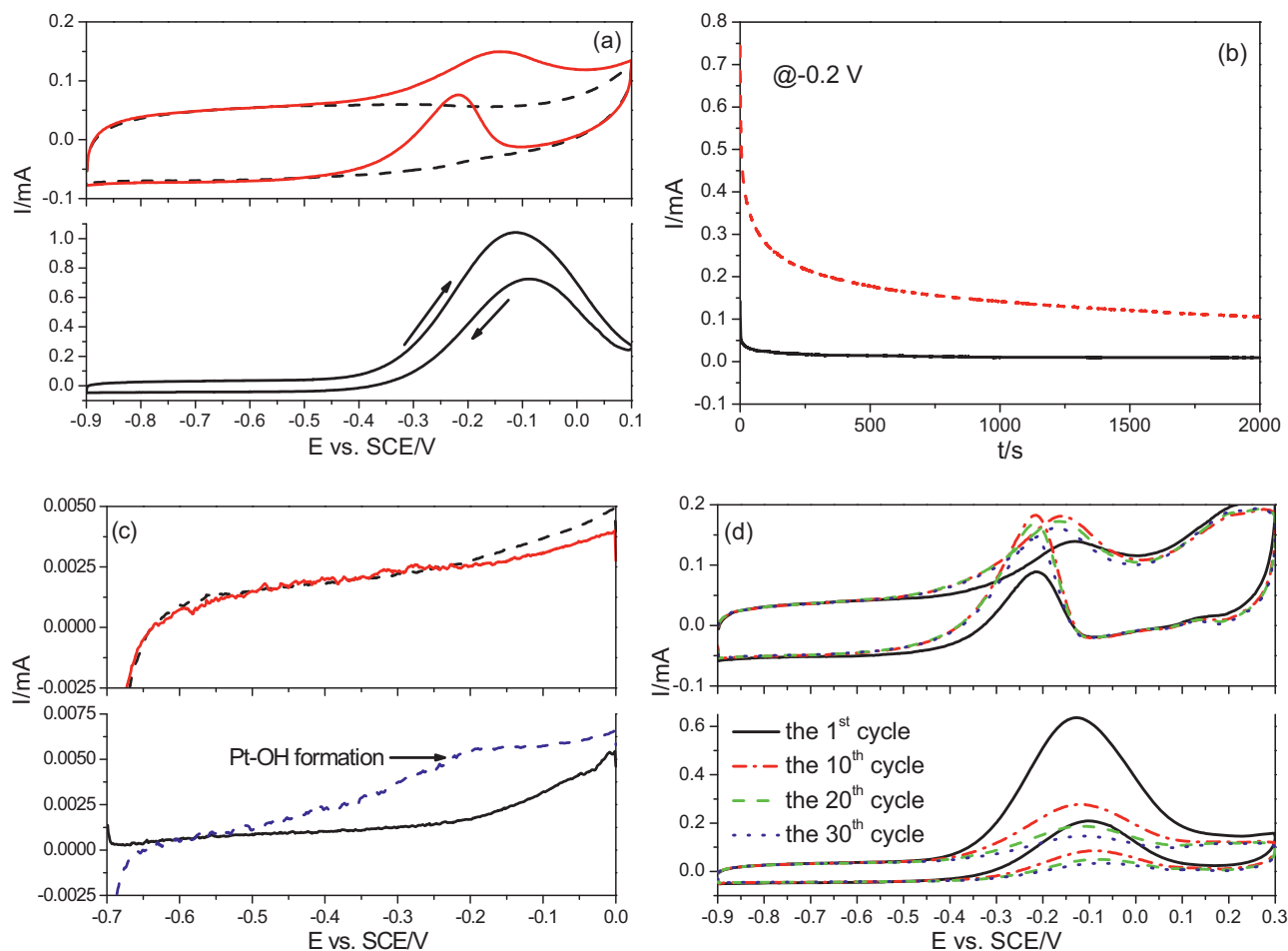


Fig. 3. (a) Cyclic voltammograms of Au/CNTs (black dash line), Pt-on-Au/CNTs (black solid line), and Pd-on-Au/CNTs (red solid line) electrodes recorded in N_2 -saturated 1 M NaOH + 1 M CH_3OH ; (b) Chronoamperometry data for Pt-on-Au/CNTs (red dash line) and Pd-on-Au/CNTs (black solid line) recorded at -0.2 V in N_2 -saturated 1 M NaOH + 1 M CH_3OH ; (c) Linear sweeping voltammetry (LSV) curves recorded on Pt-on-Au/CNTs (blue dash line in lower graph) and Pd-on-Au/CNTs (red solid line in upper graph) in N_2 -saturated 1 M NaOH together with corresponding curve for Au/CNTs. Potential scan rate: 0.002 V s^{-1} . (d) Variation of methanol oxidation peak current with CV cycling on Pt-on-Au/CNTs (lower graph) and Pd-on-Au/CNTs (upper graph) recorded in N_2 -saturated 1 M NaOH + 1 M CH_3OH .

the OH_{ad} plays a crucial role on MOR process according to the bi-functional mechanism [26], the more facile formation of Pt-OH in Pt-on-Au/CNTs certainly results in a higher activity for methanol oxidation reaction.

However, the stability of Pt-on-Au catalysts is low and the peak current of MOR sharply decreases with increasing CV cycling (see lower graph in Fig. 3(d)). In contrast, the Pd-on-Au/CNTs shows less loss of methanol oxidation peak current with the CV cycling (see upper graph in Fig. 3(d)), indicating a higher stability of Pd than Pt. Based on these results, we have further studied the possibility to modify Pd with Pt to achieve both higher activity and stability (Section 3.2).

3.2. Preparation of Pt-on-Pd-on-Au/CNTs and Pt-on-Pd/CNTs to improve the Pt stability and Pd activity simultaneously

To modify Pd with Pt via the Pt-on-Pd structure, Pd substrate was firstly prepared by depositing Pd on CNTs-supported Au and then Pt was deposited on Pd surface. The obtained material was denoted as Pt-on-Pd-on-Au/CNTs for following characterization.

Fig. 4(a) reflects the structural changes with Pd deposition (4000 seconds) on Au and then Pt deposition (20 seconds) on Pd. It can be seen that the intensity of Au oxide reduction peak is greatly decreased after Pd deposition, demonstrating a high coverage of Pd on Au. At the same time, a new peak at 0.7 V ascribed to Pd oxide

reduction [37] confirms the formation of Pd-on-Au structure. In ref. 37 the Pd-OH reduction peak lies in 0.6 V vs. Ag/AgCl electrode. The reason why our Pd peak lies in a higher value (0.7 V vs. SCE) is that the CV scanning rate is low and the Pd amount is small. As we know, increasing the CV scanning rate would influence the peak location, since our rate is 0.05 V s^{-1} while the rate in ref. 37 is 0.5 V s^{-1} , the deviation of peak location is understandable. After Pt deposition followed, the intensity of Pd oxide reduction peak is significantly decreased and a new peak at 0.5 V appears, which can be ascribed to Pt oxide reduction [37]. It is noteworthy that the Au peak intensity does not see a decrease after Pt deposition, indicating that the Pt moieties only deposits on Pd other than Au surface and the Pt amount must be too low to stretch the Pt entities to the Au surface.

Fig. 4(b) shows the activity of methanol oxidation on different catalysts, namely, Au/CNTs, Pd-on-Au/CNTs and Pt-on-Pd-on-Au/CNTs. It can be seen that the peak current for methanol oxidation is highly improved on Pt-on-Pd-on-Au/CNTs in comparison with that on Pd-on-Au/CNTs and the onset potential (E_{onset}) shifts to a lower value. This can be explained from the aspect of the facile Pt-OH formation. As seen from the inset graph in Fig. 4(b), a broad peak appears for the formation of Pt-OH and the peak current is evidently higher. In contrast to this, the peak for Pd-OH formation (see the red arrow) is quite smaller and the corresponding peak current is quite lower. From this result we conclude that Pt

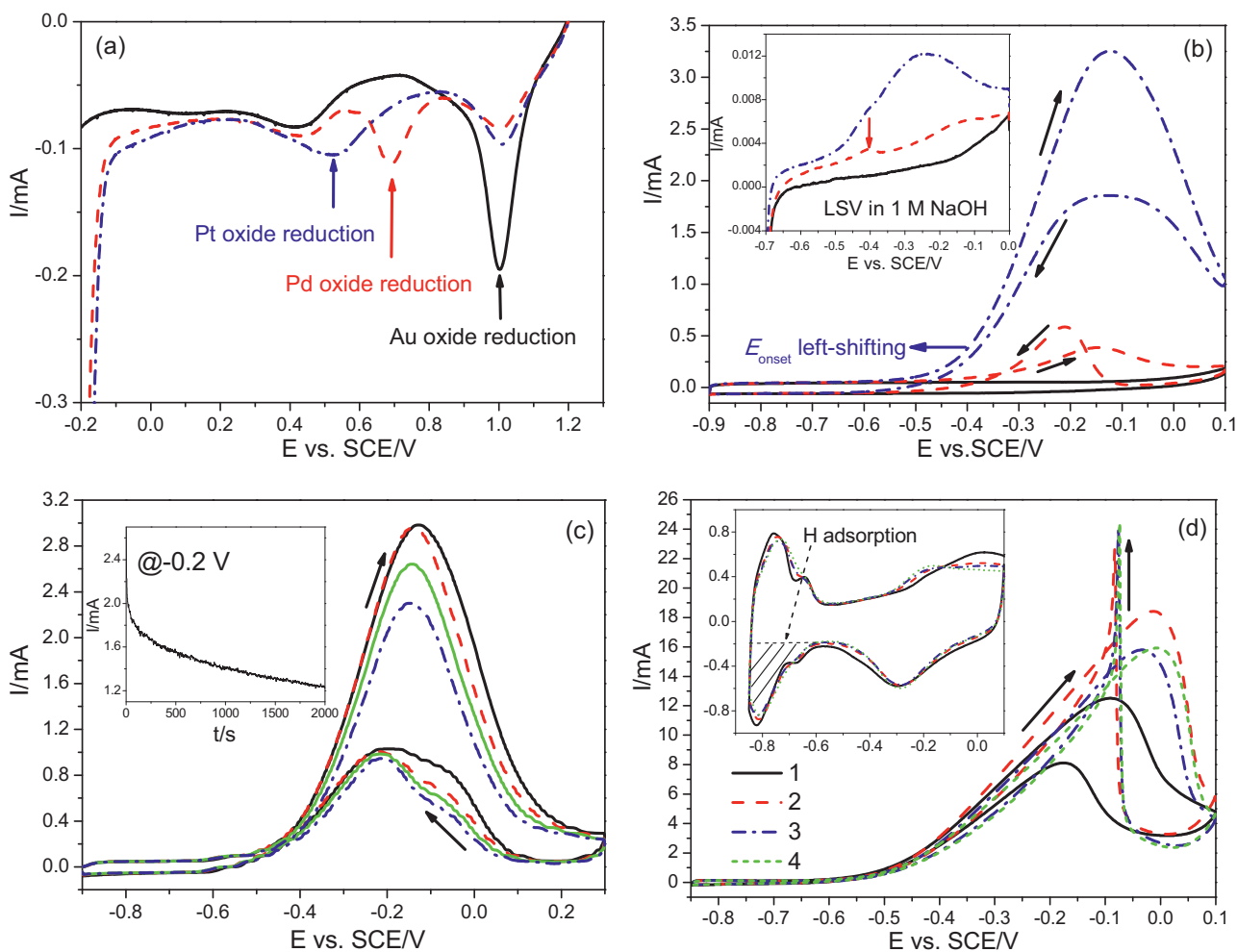


Fig. 4. (a) LSV curves of Au/CNTs (black solid line), Pd-on-Au/CNTs (red dash line) and Pt-on-Pd-on-Au/CNTs (blue dash dot line) recorded in N_2 -saturated 1 M $HClO_4$. Potential scan rate: $0.05 V s^{-1}$; (b) CVs recorded on Au/CNTs (black solid line), Pd-on-Au/CNTs (red dash line) and Pt-on-Pd-on-Au/CNTs (blue dash dot line) in N_2 -saturated 1 M NaOH + 1 M CH_3OH . The inset shows corresponding LSV curves recorded in N_2 -saturated 1 M NaOH at $0.002 V s^{-1}$; (c) Methanol oxidation peak current with 1st (solid black line), 10th (red dash line), 20th (solid green line) and 30th (blue dash dot line) cycle of CV scanning on Pt-on-Pd-on-Au/CNTs recorded in N_2 -saturated 1 M NaOH + 1 M CH_3OH . The inset shows the corresponding chronoamperometry data; (d) CVs recorded on (1) Pt/CNTs, (2) Pd-on-Pt/CNTs (5 s), (3) Pd-on-Pt/CNTs (10 s) and (4) Pd-on-Pt/CNTs (15 s) in N_2 -saturated 1 M NaOH + 1 M CH_3OH . The inset shows corresponding CVs recorded in N_2 -saturated 1 M NaOH. The theoretical loading Pt/CNTs is 0.1 mg.

enhances the methanol oxidation activity of Pd most possibly through the facile formation of Pt-OH. To gain an insight of the rough composition of Pt-on-Pd-on-Au/CNTs, we calculated the Pd mass to be about 4.4×10^{-4} mg based upon the electro-deposition current and time (result not shown). For the Pt mass calculation using the same method, we admit the result is inaccurate because a reliable average deposition current cannot be obtained within this short time range. However, because the Pt mass is too low to be detected using inductively coupled plasma (ICP) method, the Pt mass (1.1×10^{-5} mg) calculated from the electro-deposition charge can indeed provide a rough reference. Based upon the Pd and Pt mass calculation and theoretical Au loading (0.02 mg) on electrode, we roughly calculated the Pt/Pd mass ratio to be about 1/40 while the Pd/Au mass ratio 1/45. Considering the quite low Pt content, the greatly increased MOR current after Pt modification on Pd confirmed the high efficiency of Pt component. The total mass activity for the Pt-on-Pd-on-Au/CNTs was calculated to be $147 mA mg_{(Au+Pd+Pt)}^{-1}$, higher than the total mass activity of Pt-on-Au/CNTs.

The stability of Pt-on-Pd-on-Au/CNTs was also characterized, as shown in Fig. 4(c). It can be seen that there is nearly no loss of peak current for the 1st and the 10th cycle, in sharp contrast to the case of the Pt-on-Au/CNTs (see Fig. 3(d)). The chronoamperometry data

for methanol oxidation also proved the excellent performance of Pt-on-Pd-on-Au/CNTs. After 2000 seconds of constant potential ($-0.2 V$) posed on Pt-on-Pd-on-Au/CNTs, the ending current is still quite high ($\sim 1.25 mA$), indicating less chance of accumulation of strongly adsorbed intermediates in alkaline media.

As shown in Fig. 4(b), introducing Pt can greatly improve the activity of Pd for methanol oxidation reaction. Can this effect be only ascribed to Pt without the Pd involvement? To check if the Pd was involved in this MOR catalysis, we deposited Pd on Pt/CNTs catalysts with deposition time periods of 5, 10 and 15 seconds by following the same procedure as preparing Au-on-Pt/CNTs [26] to obtain three catalysts. For these catalysts, there is little difference of electrochemical active surface area, as can be seen from the H adsorption region in the inset in Fig. 4(d), indicating the Pd deposition amounts are low on Pt surface. However, the activities for methanol oxidation reaction on these three Pd-on-Pt/CNTs catalysts are all improved when compared with Pt/CNTs (Fig. 4(d)). It is worthwhile to note that the Pt surfaces in the Pd-on-Pt/CNTs catalysts are covered by Pd entities, a "less active" component in producing OH_{ad} in comparison with Pt. From the fact that the methanol oxidation activity does not decrease but increase after "less active" Pd covering Pt, it can be deduced that Pd component plays a unique role other than providing Pd-OH. According to the

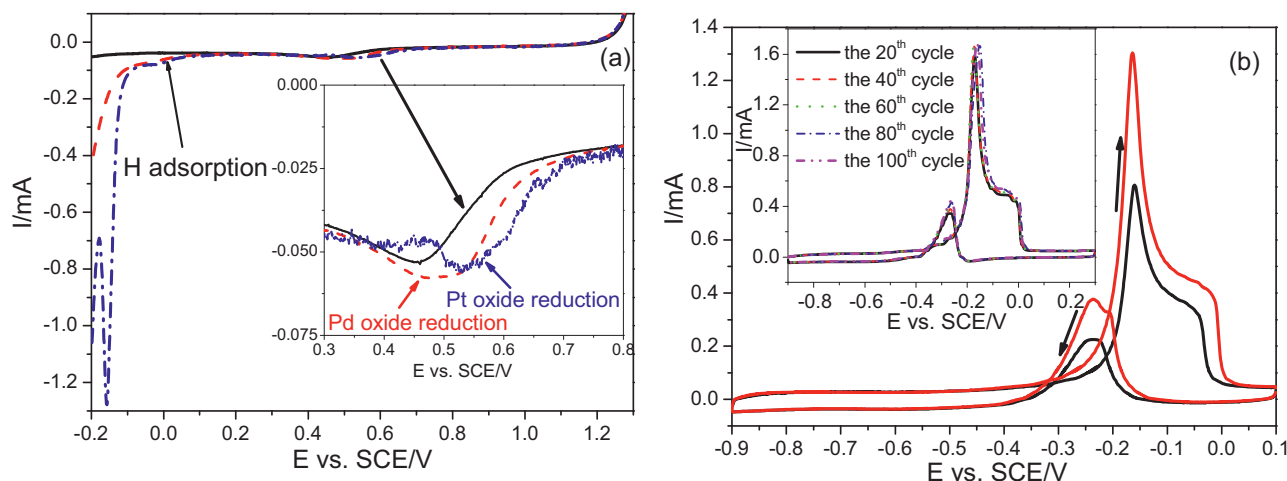


Fig. 5. (a) LSV curves of CNTs (solid black line), Pd/CNTs (red dash line) and Pt-on-Pd/CNTs (blue dash dot line) recorded in N_2 -saturated 1 M $HClO_4$. Potential scan rate: $0.05 V s^{-1}$. The inset shows the enlarged part for observing the Pd and Pt oxide reduction; (b) CVs recorded on Pt-on-Pd/CNTs (red line) and Pd/CNTs (black line) in N_2 -saturated 1 M $NaOH + 1 M CH_3OH$. The inset shows the variation of methanol oxidation peak current with CV sweeping on Pt-on-Pd/CNTs recorded in N_2 -saturated 1 M $NaOH + 1 M CH_3OH$.

bifunctional mechanism [26], the most possible role that Pd plays might be providing a substrate for CH_3O^- adsorption through reaction: $Pt - OH + Pd - CH_3O^- \rightarrow Pt + Pd + CH_2O + H_2O + e^-$.

Although the above results show the positive interaction between Pd and Pt, the existence of Au in Pt-on-Pd-on-Au/CNTs catalyst might undermine the readers' understanding of the effect of Pd. Considering this, we further prepared Pd/CNTs through 600 seconds of electro-deposition of Pd on CNTs and then 20 seconds of Pt deposition on Pd. According to the deposition currents and time (results not shown here), the Pd mass was calculated to be $2.25 \times 10^{-3} mg$ while the Pt mass was not calculated because the difference between deposition current and the blank current is too small. The formation of thus prepared Pd/CNTs can be confirmed from an evident H adsorption current (Fig. 5(a)) and a peak ascribed to Pd oxide reduction (see the inset in Fig. 5(a)). After Pt deposition on Pd/CNTs to form Pt-on-Pd/CNTs, the H adsorption current is increased significantly because of the high activity of Pt for H adsorption. At the same time, the intensity of Pd oxide reduction peak decreases and a new peak related to Pt oxide reduction appears, confirming the formation of Pt-on-Pd structure.

The activity of Pt-on-Pd/CNTs for methanol oxidation reaction was then characterized in comparison with that of Pd/CNTs. The peak current for methanol oxidation on Pt-on-Pd/CNTs (1.3 mA) is evidently higher than that on Pd/CNTs (0.8 mA) (see Fig. 5(b)), and the E_{onset} also shifts to a lower value, which is similar to the case where Pt-on-Pd-on-Au/CNTs shows much higher activity than Pd-on-Au/CNTs (see Fig. 4(b)). These results indicate that the Pd activity can be enhanced by Pt component. Besides, the peak current drop of methanol oxidation reaction is insignificant after 100 cycles of CV cycling (see the inset in Fig. 5(b)), indicating an excellent stability of Pt-on-Pd/CNTs. On the other hand, the Pd mass activity for Pd/CNTs was calculated to be $\sim 356 mA mg_{Pd}^{-1}$, the total mass activity for Pt-on-Pd/CNTs was calculated to be $\sim 578 mA mg_{(Pd+Pt)}^{-1}$, and the mass activity of Pt/CNTs was calculated to be $\sim 625 mA mg_{Pt}^{-1}$ from Fig. 4(d). The difference between mass activity of Pt-on-Pd/CNTs and Pt/CNTs is small (7.5%), indicating the promising potential of Pt-on-Pd as low-Pt catalysts for methanol oxidation catalysis.

In summary, a synergistic interaction between Pd and Pt in terms of methanol oxidation was demonstrated. The key role of Pt during methanol oxidation reaction might be to provide Pt-OH and Pd might act as adsorption site for alkoxide (CH_3O^-). At the same time, the Pt stability can be improved by depositing Pt on Pd surface. Although the mechanism for the improved stability of

Pt-on-Pd in contrast to Pt-on-Au is still unclear, we believe the catalyst with Pt-on-Pd structure is competitive in terms of activity, stability and overall cost.

4. Conclusions

Electrochemical comparison between Pt-on-Au/CNTs and Pd-on-Au/CNTs showed that Pt is more active for methanol oxidation while Pd is more stable. Considering this, Pt-on-Pd/CNTs catalyst was electrochemically prepared exhibiting higher methanol oxidation activity than Pd/CNTs and higher stability than Pt-on-Au/CNTs. The composition of Pt-on-Pd catalysts was roughly analyzed and the total mass activity of composite catalysts was calculated, showing that modifying Pd surface with low amount of Pt might be a reliable strategy to develop economic catalysts for methanol oxidation.

Acknowledgments

This research is financially supported by the National Natural Science Foundation of China (U1304215) and the China Scholarship Council.

References

- [1] M.N. Banis, S.H. Sun, X.B. Meng, Y. Zhang, Z.Q. Wang, R.Y. Li, M. Cai, T.K. Sham, X. L. Sun, $TiSi_2O_x$ coated N-Doped carbon nanotubes as Pt catalyst support for the oxygen reduction reaction in PEMFCs, *J. Phys. Chem. C* 117 (2013) 15457.
- [2] S. Cavaliere, S. Subianto, I. Savych, M. Tillard, D.J. Jones, J. Roziere, Dopant-driven nanostructured loose-tube SnO_2 architectures: alternative electro-catalyst supports for proton exchange membrane fuel cells, *J. Phys. Chem. C* 117 (2013) 18298.
- [3] J.T. Wang, X.J. Yue, Z.Z. Zhang, Z. Yang, Y.F. Li, H. Zhang, X.L. Yang, H. Wu, Z.Y. Jiang, Enhancement of proton conduction at low humidity by incorporating imidazole microcapsules into polymer electrolyte membranes, *Adv. Funct. Mater.* 22 (2012) 4539.
- [4] Q.X. Wu, S.Y. Shen, Y.L. He, T.S. Zhao, Effect of water concentration in the anode catalyst layer on the performance of direct methanol fuel cells operating with neat methanol, *Int. J. Hydrogen Energ.* 37 (2012) 5958.
- [5] Z.Y. Shih, C.W. Wang, G.B. Xu, H.T. Chang, Porous palladium copper nanoparticles for the electrocatalytic oxidation of methanol in direct methanol fuel cells, *J. Mater. Chem. A* 1 (2013) 4773.
- [6] Z.H. Zhang, C. Zhang, J.Z. Sun, T.Y. Kou, Q.G. Bai, Y. Wang, Y. Ding, Ultrafine nanoporous PdFe/Fe $3O_4$ catalysts with doubly enhanced activities towards electro-oxidation of methanol and ethanol in alkaline media, *J. Mater. Chem.* 1 (2013) 3620 A.
- [7] C.J. Pelliccione, E.V. Timofeeva, J.P. Katsoudas, C.U. Segre, In situ Ru K-Edge x-ray absorption spectroscopy study of methanol oxidation mechanisms on model submonolayer Ru on Pt nanoparticle electrocatalyst, *J. Phys. Chem. C* 117 (2013) 18904.

- [8] A.V. Miller, V.V. Kaichev, I.P. Prosvirin, V.I. Bukhtiyarov, Mechanistic study of methanol decomposition and oxidation on Pt(111), *J. Phys. Chem. C* 117 (2013) 8189.
- [9] C.Y. He, J.J. Zhang, P.K. Shen, Nitrogen-self-doped graphene-based non-precious metal catalyst with superior performance to Pt/C catalyst toward oxygen reduction reaction, *J. Mater. Chem. A* 2 (2014) 3231.
- [10] G.Q. He, Y. Song, K. Liu, A. Walter, S. Chen, S.W. Chen, Oxygen reduction catalyzed by platinum nanoparticles supported on graphene quantum dots, *ACS Catal.* 3 (2013) 831.
- [11] J.M. Yang, S.A. Wang, C.L. Sun, M.D. Ger, Synthesis of size-selected Pt nanoparticles supported on sulfonated graphene with polyvinyl alcohol for methanol oxidation in alkaline solutions, *J. Power Sources* 254 (2014) 298.
- [12] M. Asgari, M.G. Maragheh, R. Davarkhah, E. Lohrasbi, A.N. Golikand, Electro-catalytic oxidation of methanol on the nickel–cobalt modified glassy carbon electrode in alkaline medium, *Electrochim. Acta* 59 (2012) 284.
- [13] A.V. Tripkovic, K.D. Popovic, B.N. Grgur, B. Bliznac, P.N. Ross, N.M. Markovic, Methanol electrooxidation on supported Pt and PtRu catalysts in acid and alkaline solutions, *Electrochim. Acta* 47 (2002) 3707.
- [14] P. Quaino, N.B. Luque, R. Nazmutdinov, E. Santos, W. Schmickler, Why is gold such a good catalyst for oxygen reduction in alkaline media, *Angew. Chem. Int. Ed.* 51 (2012) 12997.
- [15] J. Yin, Y.J. Qiu, J. Yu, X.S. Zhou, W.H. Wu, Enhancement of electrocatalytic activity for oxygen reduction reaction in alkaline and acid media from electrospun nitrogen-doped carbon nanofibers by surface modification, *RSC Adv.* 3 (2013) 15655.
- [16] Y.J. Wang, J.L. Qiao, R. Baker, J.J. Zhang, Alkaline polymer electrolyte membranes for fuel cell applications, *Chem. Soc. Rev.* 42 (2013) 5768.
- [17] J. Pan, C. Chen, L. Zhuang, J.T. Lu, Designing advanced alkaline polymer electrolytes for fuel cell applications, *Acc. Chem. Res.* 45 (2012) 473.
- [18] O.I. Deavin, S. Murphy, A.L. Ong, S.D. Poynton, R. Zeng, H. Herman, J.R. Varcoe, Anion-exchange membranes for alkaline polymer electrolyte fuel cells: comparison of pendent benzyltrimethylammonium- and benzylmethylimidazolium-head-groups, *Energy Environ. Sci.* 5 (2012) 8584.
- [19] S. Cherevko, N. Kulyk, C.H. Chung, Utilization of surface active sites on gold in preparation of highly reactive interfaces for alcohols electrooxidation in alkaline media, *Electrochim. Acta* 69 (2012) 190.
- [20] Y.Y. Xu, Y.N. Dong, J. Shi, M.L. Xu, Z.F. Zhang, X.K. Yang, Au@Pt core-shell nanoparticles supported on multiwalled carbon nanotubes for methanol oxidation, *Catal. Commun.* 13 (2011) 54.
- [21] Q. Tan, C.Y. Du, G.P. Yin, P.J. Zuo, X.Q. Cheng, M. Chen, Highly efficient and stable nonplatinum anode catalyst with Au@Pd core-shell nanostructures for methanol electrooxidation, *J. Catal.* 295 (2012) 217.
- [22] A. Safavi, H. Kazemi, S.H. Kazemi, In situ electrodeposition of graphene/nanopalladium on carbon cloth for electrooxidation of methanol in alkaline media, *J. Power Sources* 256 (2014) 354.
- [23] M. Sawangphruk, A. Krittayavathananon, N. Chinwipas, P. Srimuk, T. Vatanatham, S. Limtrakul, J.S. Foord, Ultraporous palladium supported on graphene-coated carbon fiber paper as a highly active catalyst electrode for the oxidation of methanol, *Fuel Cell* 13 (2013) 881.
- [24] M.M. Liu, Y.Z. Lu, W. Chen, PdAg nanorings supported on graphene nanosheets: highly methanol-tolerant cathode electrocatalyst for alkaline fuel cells, *Adv. Funct. Mater.* 23 (10) (2013) 1289.
- [25] M.Y. Jing, L.H. Jiang, B.L. Yi, G.Q. Sun, Comparative study of methanol adsorption and electro-oxidation on carbon-supported platinum in acidic and alkaline electrolytes, *J. Electroanal. Chem.* 688 (2013) 172.
- [26] J.S. Wang, R.R. Shi, X. Guo, J.Y. Xi, J.H. Zhao, C.Y. Song, L.C. Wang, J.J. Zhang, Highly active Pt-on-Au catalysts for methanol oxidation in alkaline media involving a synergistic interaction between Pt and Au, *Electrochim. Acta.* 123 (2014) 309.
- [27] J.T. Zhang, P.P. Liu, H.Y. Ma, Y. Ding, Nanostructured porous gold for methanol electro-oxidation, *J. Phys. Chem. C* 111 (2007) 10382.
- [28] C.W. Xu, Y.L. Liu, D.S. Yuan, Pt and Pd supported on carbon microspheres for alcohol electrooxidation in alkaline media, *Inter. J. Electrochem. Sci.* 2 (2007) 674.
- [29] Z. Yin, Y.N. Zhang, K. Chen, J. Li, W.J. Li, P. Tang, H.B. Zhao, Q.J. Zhu, X.H. Bao, D. Ma, Monodispersed bimetallic PdAg nanoparticles with twinned structures: Formation and enhancement for the methanol oxidation, *Sci. Rep.* 4 (2014) 4288, doi:<http://dx.doi.org/10.1038/srep04288>.
- [30] M. Zhao, K. Abe, S. Yamaura, Y. Yamamoto, N. Asao, Fabrication of Pd–Ni–P metallic glass nanoparticles and their application as highly durable catalysts in methanol electro-oxidation, *Chem. Mater.* 26 (2014) 1056.
- [31] Y.S. Li, T.S. Zhao, Understanding the performance degradation of anion-exchange membrane direct ethanol fuel cells, *Int. J. Hydrogen Energ.* 37 (2012) 4413.
- [32] J.S. Wang, J.Y. Xi, L. Zhang, J.J. Zhang, X. Guo, J.H. Zhao, C.Y. Song, L.C. Wang, Synthesis of highly active SnO₂-CNTs supported Pt-on-Au composite catalysts through site-selective electrodeposition for HCOOH electrooxidation, *Electrochim. Acta* 112 (2013) 480.
- [33] S. Ghosh, R.K. Sahu, C.R. Raj, Pt–Pd alloy nanoparticle-decorated carbon nanotubes: a durable and methanol tolerant oxygen reduction electrocatalyst, *Nanotechnology* 23 (2012) 385602.
- [34] H. Wang, S. Ji, W. Wang, R.F. Wang, Amorphous Pt@PdCu-CNT catalyst for methanol electrooxidation, *S. Afr. J. Chem.* 66 (2013) 17.
- [35] J.S. Wang, X. Guo, C.Y. Song, L.C. wang, J.H. Zhao, X.P. Qiu, Promoting methanol electro-oxidation through fabricating pore structure in Pt/CNTs catalyst layer by dissolving away premixed La₂O₃ particles, *Acta Phys. Chim. Sin.* 25 (2009) 767.
- [36] J.H. Zhu, J.J. Wu, F. Liu, R.J. Xing, C.Z. Zhang, C. Yang, H. Yin, Y.L. Hou, Controlled synthesis of FePt–Au hybrid nanoparticles triggered by reaction atmosphere and FePt seeds, *Nanoscale* 5 (2013) 9141.
- [37] M. Ahn, J.W. Kim, Insights into the electrooxidation of formic acid on Pt and Pd shells on Au core surfaces via SERS at dendritic Au rod electrodes, *J. Phys. Chem. C* 117 (2013) 24438.